

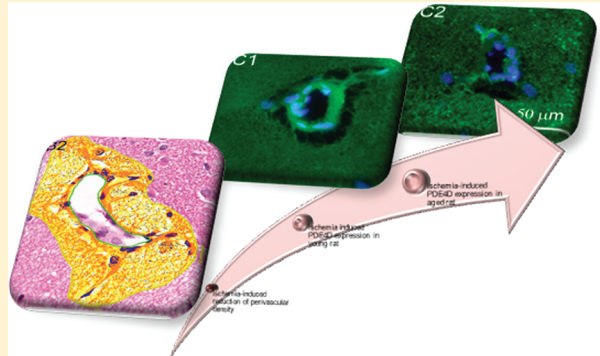
# Ischemia-Induced Increase in Microvascular Phosphodiesterase 4D Expression in Rat Hippocampus Associated with Blood Brain Barrier Permeability: Effect of Age

Zhen He,<sup>†,‡</sup> Bei He,<sup>‡</sup> Brian L Behrle,<sup>‡</sup> M. Phillip C. Fejleh,<sup>‡</sup> Li Cui,<sup>\*,‡</sup> Merle G. Paule,<sup>†</sup> and L. John Greenfield<sup>‡</sup>

<sup>†</sup>Division of Neurotoxicology, National Center for Toxicological Research, Food and Drug Administration, Silver Spring, Maryland 20993, United States

<sup>‡</sup>Department of Neurology, University of Arkansas for Medical Sciences, Little Rock, Arkansas 72205, United States

**ABSTRACT:** Phosphodiesterase 4D (PDE4D) is one of 16 PDEs expressed in cerebral microvessels, and may be involved in regulating blood-brain barrier (BBB) permeability. To assess the possible role of PDE4D in stroke-related injury in young versus aged rats, we measured microvascular PDE4D expression, parenchymal albumin immunoreactivity, and changes in the inside bore of the brain microvasculature. Ischemia caused severe hippocampal CA1 damage, associated with significant increases in vascular PDE4D and parenchymal albumin immunoreactivities. This effect was greater in the younger animals, which also had a greater increase in PDE4D expression. Ischemia significantly decreased tissue density in the perimicrovascular space in both young and aged animals. In addition, internal bore circumference and cross-sectional area of the hippocampal microvessels increased dramatically following ischemia. Increased PDE4D expression following cerebral ischemia may play a role in changing BBB permeability, which could secondarily affect ischemic outcome.



**KEYWORDS:** Aging, microvascular PDE4D, parenchymal albumin, perimicrovascular space, rat hippocampus, transient global ischemia

Recently, we demonstrated that 16 PDE superfamily members are expressed at the transcriptional level in cerebral microvessels.<sup>1</sup> Furthermore, PDE4D immunoreactivity was colocalized in brain microvessels with the endothelial marker, rat endothelial cell antigen-1 (RECA-1) and the vascular machinery marker,  $\alpha$ -smooth muscle actin ( $\alpha$ -SMA).<sup>1</sup> The proximity of PDE4D to these markers suggests the possibility that PDE4D may participate in regulating microcirculation and affect the permeability of the brain-blood barrier (BBB).

The present study attempts to explore possible roles that PDE4D may play in the acute phase of cerebral ischemia by simultaneously examining PDE4D expression and ischemic damage as evidenced by hippocampal cell death and changes in density in perimicrovascular space and in parenchymal immunoreactivity of albumin, which have been linked to changes in BBB permeability.<sup>2</sup>

Rats subjected to global ischemia using the four-vessel-occlusion model suffered severe neuron loss in the hippocampal CA1 region, consistent with our previous studies.<sup>3,4</sup> The living cell ratio, defined as the ratio of live CA1 neurons in the postischemic animals to that found in controls, was higher in the aged than in the young ischemic group (Figure 1A1, A2, B1), indicating more neuron loss in the hippocampal CA1

region of the young ischemic group than in the aged ischemic group. The age-related difference in cell survival may result from distinct pathogenic cell death mechanisms: in young adults, it appears that necrosis predominates, while in aged animals cell death is delayed and likely due to apoptosis.<sup>3,4</sup> The young animals displayed a higher level of microvascular PDE4D expression than observed in older animals following cerebral ischemia (Figure 1B2, C1, and C2), which inversely correlated with CA-1 cell survival. Transient global ischemia induced a significant increase in PDE4D immunoreactivity in hippocampal microvessels in both young (4.8-fold) and aged (1.7-fold) animals, compared with their controls. There was no detectable difference in PDE4D immunoreactivity between young and aged rats subjected to sham surgery. The higher PDE4D increase in younger animals correlated with lower living cell ratio in area CA-1 than seen in older animals, which had only a small increase in PDE4D and higher CA1 cell survival.

The decrease in cell survival associated with increased PDE4D in younger animals may have been due to changes in BBB permeability. As demonstrated in Figure 2A1 and A2, the perimicrovascular space in young animals subjected to sham

**Published:** February 27, 2012

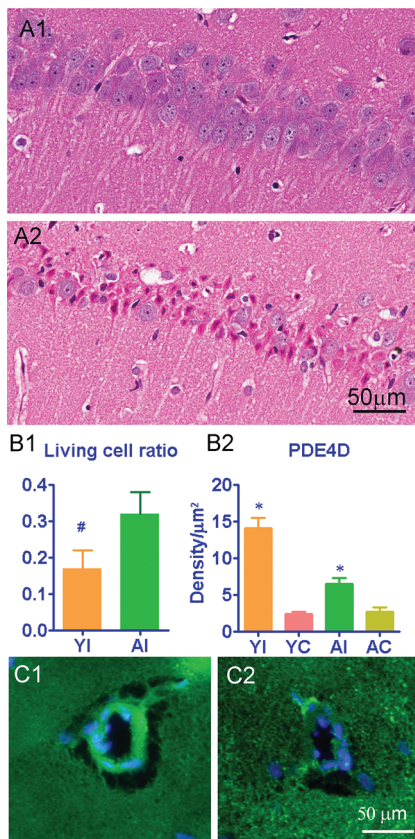


**Figure 1.** Living cell ratios (ischemic/control) inversely correlate with intensity of PDE4D immunoreactivity following transient global ischemia. Panels A and B show the hippocampal CA1 region, sham surgery (A1) vs ischemia (A2) in young animals. The living cell ratio in the hippocampal CA1 region was significantly higher in the aged group than in young group following transient global ischemia (B1). There were very low PDE4D immunoreactivities in both young and aged rats subjected to sham surgery (B2) but ischemia induced a significant increase in the PDE4D immunoreactivity in both young (B2, C1) and aged (B2, C2) rats. AC = aged control groups; AI = aged ischemic group; YC = young control group; YI = young ischemic group;  $^{\#}p < 0.05$ , AC vs YC;  $*p < 0.05$ , AI vs AC or YI vs YC.

surgery displayed homogeneously and densely distributed parenchymal matrix/neuropil. Cerebral ischemia resulted in reduced density of the perimicrovascular space (Figure 2B1, B2) in both young and aged animals (Figure 2C1). The ischemia-induced reduction in tissue density was associated with a dramatic increase in the internal bore circumference and cross-sectional area of the hippocampal microvessel lumens (Figure 2C2). Again, young animals displayed a larger reduction in tissue density and increase in microvessel dimensions than older animals after ischemia, correlating with the greater increase in PDE4D expression. Interestingly, the average perimicrovascular tissue density along the hippocampal fissure in the aged sham surgery group was significantly lower than in the young sham surgery group (Figure 2C1), suggesting age-related differences in BBB permeability.

This is the first description of changes in microvascular PDE4D expression following cerebral ischemia. There is very limited information linking PDE4D function to cerebral ischemia. BBB022P, a PDE4 inhibitor, has been shown to protect against BBB disruption, but the issue of cell death in focal cerebral ischemia was not addressed.<sup>5</sup> PDE4 blockade of BBB disruption is consistent with our results in transient global

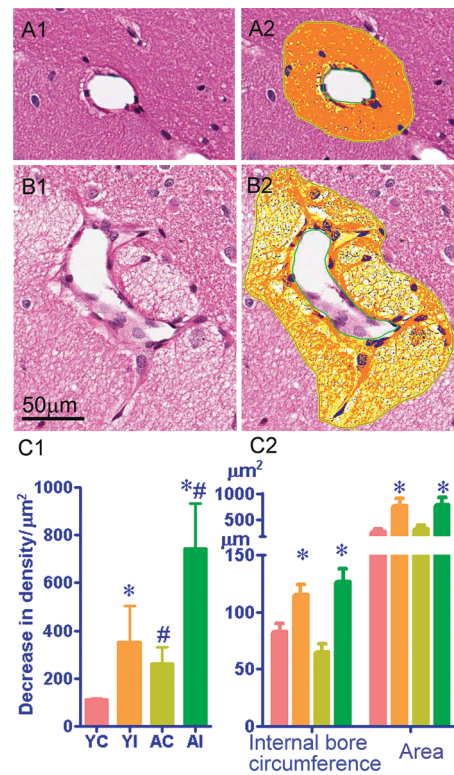


**Figure 2.** Morphological changes in hippocampal microvessels. Panel A shows a perivascular brain region for a single microvessel (A1) with the perivascular tissue density identified by perivascular positive pixel counting (A2) in the sham surgery condition in a young rat. Similarly, panel B demonstrates the perivascular densities in the same microvessel before (B1) and after (B2) perivascular positive pixel counting in the ischemic condition. Aged rats showed significantly reduced perimicrovascular density as compared with young animals following sham surgery ( $p < 0.05$ , Figure 2C1). Ischemia resulted in reduced perimicrovascular density as compared with sham surgery groups in both young and aged groups. Ischemia significantly increased the internal bore circumference and cross-sectional area of microvessel lumens (C2). AC = aged control group; AI = aged ischemic group; YC = young control group; YI = young ischemic group;  $n = 14–23$  microvessels/animal;  $^{\#}p < 0.05$ , AC vs YC or AI vs YI;  $*p < 0.05$ , AI vs AC or YI vs YC.

ischemia, demonstrating an increase in PDE4D (Figure 1B2) correlating with a persistent reduction in density of the perimicrovascular space (Figure 2C1), suggesting a compromised BBB.<sup>2</sup> However, PDE4 inhibitors may block both PDE4A and PDE4D. At the transcriptional level, PDE4A is expressed to a much higher degree (~8 times) than PDE4D in intact brain microvessels.<sup>1</sup> Thus, the PDE4 inhibitor results may be relevant to the current studies but do not rule out contributions from other PDE isoforms.

Leakage of serum protein and/or accumulation of macrophages/white blood cells into brain have been reported in humans<sup>6</sup> with small vessel disease and animal models of pericyte-deficiency.<sup>7</sup> Such observations are likely to be at least partially attributable to age-associated increases in BBB permeability. Increases in BBB permeability have been reported to occur shortly following the onset of transient global ischemia.<sup>8–10</sup> Entry of serum proteins into the perivascular space and brain parenchyma may elicit immunological, biochemical, and metabolic reactions leading to vasogenic brain edema.<sup>11</sup>

To determine whether increased microvessel size and decreased perivascular tissue density after ischemia are in fact due to BBB disruption and associated entry of serum proteins into the perivascular space, we also measured the density of albumin in perivascular brain regions before and after ischemia. As demonstrated in Figure 3, parenchymal albumin immunoreactivity was significantly higher in ischemic groups than in both young and aged sham surgery groups.

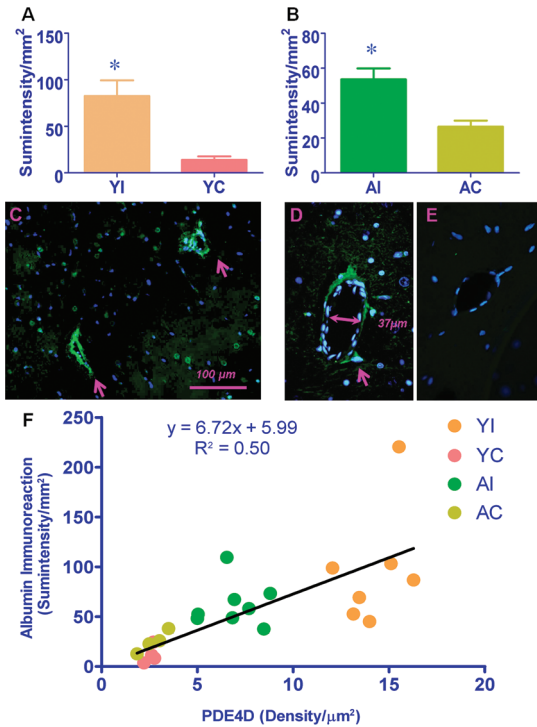


**Figure 3.** Parenchymal albumin-immunoreactivity in the hippocampus. Panels A and B show parenchymal albumin immunoreactivity before and after cerebral ischemia in young (A) and aged (B) groups, respectively. Parenchymal albumin immunoreactivity was significantly higher in ischemic groups than in both young and aged sham surgery groups. Notably, deposits of albumin-immunoreactivity were often observed in the perimicrovascular space in the ischemic groups (C and D), but not in the control groups (E). Linear regression of parenchymal albumin-immunoreactivity on the *y* axis and the PDE4D immunoreactivity on the *x* axis demonstrates that PDE4D expression correlates with the albumin immunoreactivity ( $r^2 = 0.50$ , F). AC = aged control groups; AI = aged ischemic group; YC = young control group; YI = young ischemic group; \* $p < 0.05$ , AI vs AC or YI vs YC.

Activity was significantly higher in the ischemic groups than that in sham surgery groups in both young and aged animals. Notably, we often observed punctate deposits of albumin-immunoreactivity in the perimicrovascular space in postischemic animals (Figure 3C and D) but not in sham controls (Figure 3E), indicating albumin leakage due to BBB damage. Similar albumin deposits associated with increased BBB permeability have been observed previously.<sup>12</sup> The linear regression between the PDE4D immunoreactivity and the parenchymal albumin-immunoreactivity (Figure 3F) demonstrates a strong correlation ( $r^2 = 0.5$ ) between PDE4D expression and a marker of BBB permeability.

The mechanism underlying BBB leakage and albumin deposits in the perimicrovascular space surrounding microvessels in this size range (about 50  $\mu\text{m}$  diameter) remains unclear. The explanation may be related to the anatomic and physiological function of the perivascular space, which may be

involved in regulating changes in the diameter/volume of the vessel associated with contraction and dilatation. Ischemia-reperfusion induced by four-vessel occlusion followed by restoration of carotid perfusion resulted in dramatic changes in these vessels, which could drive the leakage into the perivascular space via processes associated with the hydrodynamic effects of vessel contraction and dilatation, or damage to tight junctions may allow free diffusion of larger solutes due to excessive dilatation. Future studies may address this question by directly observing living microvessels and the perivascular space during the ischemia-reperfusion process.

The discrepancy between young and aged animals in the induction of PDE4D expression, the associated reduction in perimicrovascular density and the degree of neuronal cell loss in response to transient ischemia may be due to aging-related factor(s). As shown in Figure 2, the baseline density of the perimicrovascular space in aged animals was significantly lower than that in young animals whereas the percent reduction in the perimicrovascular density following cerebral ischemia was similar in both young (120%) and aged (80%) animals. Differences in blood pressure, intracranial pressure, or vascular compliance between young and aged animals following cerebral ischemia may explain the age-related differences in response, and would be an important topic for future study.

The present study demonstrates that the microvascular PDE4D immunoreactivity correlates significantly with parenchymal albumin leakage (Figure 3F). Nevertheless, the evidence is not strong enough to establish a causal relationship between PDE4D expression and hippocampal CA1 damage following transient global ischemia: it is still not known whether hippocampal ischemic damage causes or is caused by an increase in PDE4D expression, or whether PDE4D plays any role in the pathogenic mechanisms of cerebral ischemia. Several additional approaches may better define whether a causative relationship exists between PDE4D, BBB permeability and/or ischemic damage. If ischemia-induced PDE4D leads to BBB permeability and cell death, inhibition of PDE4D expression with an agent such as rolipram following ischemia should improve ischemic outcome via reducing BBB permeability. However, such inhibitors may block all isoforms of PDE4<sup>13</sup> including PDE4A<sup>14</sup> which is much more highly expressed than PDE4D in brain microvessels.<sup>1</sup> Hence, nonselective PDE4 blockade may positively affect ischemic outcome, but would not conclusively determine which PDE4 isozyme was involved or establish a causal link between PDE4 activity and BBB permeability. Alternatively, PDE4D knockout animals would provide useful information for defining PDE4D involvement following transient global ischemia. However, the genetic deficiency of PDE4D might induce compensatory upregulation of other PDE isoforms that could complicate the response to cerebral ischemia, since there are 16 different PDEs expressed in brain microvessels.<sup>1</sup> Of these, five PDEs including PDE4D are cAMP-specific, while another five hydrolyze both cAMP and cGMP. While currently there is no report in the literature indicating that PDE4D knockout may induce other PDE gene expression or activity modification, 20% of the Eph/ephrin family genes are up-regulated after deletion of gene ephrinAS,<sup>15</sup> indicating specificity of adaptive and compensative changes in gene expression after the mutation of a single gene and complexity of interpreting phenotypes of gene knockout animals.<sup>15</sup> Additional evidence may be required to exclude one or several substituting PDEs that might respond to cerebral ischemia in PDE4D knockout animals, whether the knockout is

constitutive or conditional. Ideally, conditional knockout or transient knock-down of PDE4D in wild-type animals might avoid such compensatory changes. Finally, more selective pharmacologic inhibition of PDE4D may better define the role of this enzyme in the microvascular response to cerebral ischemia.

In conclusion, decreased perimicrovascular tissue density and enlarged microvascular bore likely indicate an increase in BBB permeability after ischemia. These changes were associated with increased PDE4D expression and increased parenchymal albumin immunoreactivity, both greater in younger animals and associated with greater neuron loss. Increased PDE4D expression following cerebral ischemia may thus play a role in changing BBB permeability and secondarily affect ischemic outcome.

## METHODS

**Animals.** Male Fischer 344 rats aged 4 months ( $n = 11$ , weighing 320–388 g) and 24 months ( $n = 12$ , weighing 380–457 g) were subjected to sham surgery ( $n = 4$  each for young and aged groups) or transient global ischemia ( $n = 7$  for young group and  $n = 8$  for aged group) and allowed to survive 8 days. Animals were housed individually and acclimated with a laboratory diet and tap water ad libitum under a fixed 12 h light/12 h dark cycle for 1–2 weeks before experimentation. Global ischemia was induced using a four-vessel-occlusion model.<sup>3,4</sup> Four young and four aged animals subjected to sham bilateral carotid artery occlusion served as controls. Institutional IACUC (Mayo Clinic Jacksonville) approved the experimental protocol.

**Histological Methods.** Animals were sacrificed under isoflurane anesthesia for histological and immunofluorescent assessments. Paraformaldehyde-PBS buffer perfused and post-mortem fixed, paraffin-embedded coronal sections (5  $\mu\text{m}$ ) were evaluated histologically using hematoxylin and eosin (H & E) staining. Digital images of the dorsal hippocampus were obtained using ScanScope CS and Aperio's ImageScope software (Aperio Technologies, Inc. Vista, CA).

**Analysis of Histological Images.** Live cell numbers/ratios from the hippocampal CA1 region were obtained using H & E stained slices as described elsewhere.<sup>3,4</sup> Briefly, living cells (normal morphology) were counted and the living cell ratio (ischemic:control) was calculated by dividing the mean living cell number in the hippocampal CA1 region per rat by the mean living cell number in the same region in sham-surgery rats of the same age. Tissue density values were determined as described previously<sup>16</sup> using positive pixel count analysis. An index [weak positive pixel count divided by (the area of the perimicrovascular tissue minus the area of the internal bore)] was used to define a reduction in the perimicrovascular tissue density. An overall average of this index was generated from the left and right hippocampi together.

**Fluorescence Methods.** Brain slices were deparaffinized and rehydrated. After blocking,<sup>1,3,4</sup> the adjacent slices were incubated with the primary anti-PDE4D antibody (ab14613: Abcam, Cambridge, MA, or alternatively sc-25814: Santa Cruz Biotechnology, Inc.; Santa Cruz, CA, diluted 1:200) or FITC tagged anti-rat albumin antibody (ab53435: Abcam, Cambridge, MA, diluted 1:50). The Alexa 488-labeled secondary antibody (Molecular Probes, Eugene, OR, diluted 1:200) was used to label the PDE4D antibody–antigen complex. 4',6-Diamidino-2-phenylindole (DAPI) was used to visualize nuclei. Negative controls employed identical procedures but substituted control rabbit IgG for the PDE4D antibody.<sup>17,18</sup>

**Analysis of Fluorescent Images.** Green or DAPI fluorescence was acquired using different camera channels equipped with filters for fluorescein isothiocyanate or DAPI. Using NIS-Element and/or NIH Image J software, fluorescence intensity was determined as described previously.<sup>18</sup> The average signal intensity (mean fluorescence intensity in arbitrary units) was determined for hippocampal microvessel PDE4D immunoreactivity (20–25 microvessels/animal) or hippo-

campal parenchymal albumin immunoreactivity and standardized per unit area (intensity/ $\mu\text{m}^2$ ) of microvascular lumen cross section.

**Statistical Analysis.** GraphPad Prism 5 (GraphPad Software, Inc. La Jolla, CA) was used to perform two-way ANOVAs with Bonferroni posthoc tests. Linear regression was used to define the correlation between parenchymal albumin immunoreactivity and microvascular PDE4D immunoreactivity. Unpaired *t* test was also used for group comparisons;  $p < 0.05$  was considered significant.

## AUTHOR INFORMATION

### Corresponding Author

\*Mailing address: Department of Neurology, University of Arkansas for Medical Sciences, 4301 West Markham Street #585, Little Rock, AR 72205. Lab phone: 501-686-5523. Office phone: 501-686-7379. E-mail: LCui@uams.edu.

### Funding

The present study was partly supported by Mayo Clinic Foundation and NCTR under Protocol # P00710 (Z.H.), NIH Grant R01-NS049389, and UAMS institutional funds (J.L.G.).

### Notes

This document has been reviewed in accordance with United States Food and Drug Administration (FDA) policy and approved for publication. Approval does not signify that the contents necessarily reflect the position or opinions of the FDA nor does mention of trade names or commercial products constitute endorsement or recommendation for use. The findings and conclusions in this report are those of the author(s) and do not necessarily represent the views of the FDA.

The authors declare no competing financial interest.

## REFERENCES

- (1) He, Z., Cui, L., Patterson, T.-A., and Paule, M.-G. (2011) Defining the phosphodiesterase superfamily members in rat brain microvessels. *ACS Chem. Neurosci.* 2, 600–607.
- (2) Wuerfel, J., Haertle, M., Waiczies, H., Tysiak, E., Bechmann, I., Wernecke, K.-D., Zipp, F., and Paul, F. (2008) Perivascular spaces—MRI marker of inflammatory activity in the brain? *Brain* 131, 2332–2340.
- (3) He, Z., Crook, J.-E., Meschia, J.-F., Brott, T.-G., Dickson, D.-W., and Mickinney, M. (2005) Aging Blunts Ischemic-Preconditioning-Induced Neuroprotection Following Transient Global Ischemia in Rats. *Curr. Neurovasc. Res.* 2, 365–374.
- (4) He, Z., Meschia, J.-F., Brott, T.-G., Dickson, D.-W., and Mickinney, M. (2006) Aging is Neuroprotective during Global Ischemia but Leads to Increased Caspase-3 and Apoptotic Activity in Hippocampal Neurons. *Curr. Neurovasc. Res.* 3, 181–186.
- (5) Belayev, L., Bustos, R., Ikeda, M., Rubin, L.-L., Kajiwara, A., Morgan, L., and Ginsberg, M.-D. (1998) Protection against blood-brain barrier disruption in focal cerebral ischemia by the type IV phosphodiesterase inhibitor BBB022: a quantitative study. *Brain Res.* 787, 277–285.
- (6) Grinberg, L.-T., and Thal, D.-R. (2010) Vascular pathology in the aged human brain. *Acta Neuropathol.* 119, 277–290.
- (7) Bell, R.-D., Winkler, E.-A., Sagare, A.-P., Singh, I., LaRue, B., Deane, R., and Zlokovic, B.-V. (2010) Pericytes control key neurovascular functions and neuronal phenotype in the adult brain and during brain aging. *Neuron* 68, 409–427.
- (8) Miclescu, A., Sharma, H.-S., Martijn, C., and Wiklund, L. (2010) Methylene blue protects the cortical blood-brain barrier against ischemia/reperfusion-induced disruptions. *Crit. Care Med.* 38, 2199–2206.
- (9) Sharma, H.-S., Miclescu, A., and Wiklund, L. (2011) Cardiac arrest-induced regional blood-brain barrier breakdown, edema formation and brain pathology: a light and electron microscopic

- study on a new model for neurodegeneration and neuroprotection in porcine brain. *J. Neural Transm.* 118, 87–114.
- (10) Pinard, E., Engrand, N., and Seylaz, J. (2000) Dynamic cerebral microcirculatory changes in transient forebrain ischemia in rats: involvement of type I nitric oxide synthase. *J. Cereb. Blood Flow Metab.* 20, 1648–1658.
- (11) Sharma, H.-S., Muresanu, D., Sharma, A., and Patnaik, R. (2009) Cocaine induced breakdown of the blood–brain barrier and neurotoxicity. *Int. Rev. Neurobiol.* 88, 297–334.
- (12) Garbuza-Davis, S., Louis, M.-K., Haller, E.-M., Derasari, H.-M., Rawls, A.-E., and Sanberg, P.-R. (2011) Blood-Brain Barrier Impairment in an Animal Model of MPS III B. *PLoS ONE* 6 (3), e16601 DOI: 10.1371/journal.pone.0016601.
- (13) Torphy, T.-J., Zhou, H.-L., Foley, J.-J., Sarau, H.-M., Manning, C.-D., and Barnette, M.-S. (1995) Salbutamol up-regulates PDE4 activity and induces a heterologous desensitization of U937 cells to prostaglandin E2. Implications for the therapeutic use of beta-adrenoceptor agonists. *J. Biol. Chem.* 270, 23598–23604.
- (14) Huston, E., Pooley, L., Julien, P., Scotland, G., McPhee, I., Sullivan, M., Bolger, G., and Houslay, M.-D. (1996) The human cyclic AMP-specific phosphodiesterase PDE-46 (HSPDE4A4B) expressed in transfected COS7 cells occurs as both particulate and cytosolic species that exhibit distinct kinetics of inhibition by the antidepressant rolipram. *J. Biol. Chem.* 271, 31334–44.
- (15) Peuckert, C., Wacker, E., Rapus, J., Levitt, P., and Bolz, J. (2008) Adaptive changes in gene expression patterns in the somatosensory cortex after deletion of ephrinA5. *Mol. Cell Neurosci.* 39, 21–31.
- (16) Cui, L., Pierce, D., Light, K.-E., Melchert, R.-B., Fu, Q., Kumar, K.-S., and Hauer-Jensen, M. (2010) Sublethal total body irradiation leads to early cerebellar damage and oxidative stress. *Curr. Neurovasc. Res.* 7, 125–135.
- (17) Cui, L., Takagi, Y., Wasa, M., Iiboshi, Y., Khan, J., Nezu, R., and Okada, A. (1997) Induction of nitric oxide synthase in rat intestine by interleukin-1alpha may explain diarrhea associated with zinc deficiency. *J. Nutr.* 127, 1729–1736.
- (18) Cui, L., Takagi, Y., Sando, K., Wasa, M., and Okada, A. (2000) Nitric oxide synthase inhibitor attenuates inflammatory lesions in the skin of zinc-deficient rats. *Nutrition* 16, 34–41.